Sustained neurotrophic factor cotreatment enhances donor and host retinal ganglion cell survival in mice

Jonathan R Soucy,[1,2] Emil Kriukov,[1,2] Julia Oswald,[1,2] John Masland,[1,2] Chris Pernstich,[3] Petr Baranov[1,2,*]

1. Department of Ophthalmology, Schepens Eye Research Institute of Mass. Eye and Ear, Boston, MA
2. Department of Ophthalmology, Harvard Medical School, Boston, MA
3. Cell Guidance Systems, Cambridge, UK

*Corresponding author: petr_baranov@meei.harvard.edu

Abstract:

Retinal ganglion cells (RGCs) lack regenerative capacity in mammals, and their degeneration in glaucoma leads to irreversible blindness. Traditional RGC transplantation has been limited by poor survival rates of transplanted cells in the hostile microenvironment of a diseased retina. Our research identifies brain-derived neurotrophic factor (BDNF) and glial-derived neurotrophic factor (GDNF) as key elements in retinal development and RGC survival through in silico analysis of the single-cell transcriptome of developing human retinas. Although these factors are abundant during development, they diminish in adulthood. Here, we demonstrate that a slow-release formulation of BDNF and GDNF enhances RGC differentiation and survival in vitro and improves RGC transplantation outcomes in mouse models. This co-treatment increased survival and

coverage of donor RGCs within the retina and enhanced neurite extension toward the optic nerve head. Lastly, this co-treatment showed neuroprotective effects on host RGCs, preserving retinal function in a model of optic neuropathy. Altogether, our findings suggest that manipulating the retinal microenvironment with slow-release neurotrophic factors holds promise in regenerative medicine for treating glaucoma and other optic neuropathies. This approach not only improves donor cell survival and integration but also provides a neuroprotective benefit to host cells, indicating a significant advancement for glaucoma therapies.

Introduction:

The loss or degeneration of retinal ganglion cells (RGCs) in glaucoma is a leading cause of irreversible blindness worldwide, with no current therapies available to restore vision once these cells are lost *(1)*. While RGCs, the neurons in the retina that relay all visual information from the eye to the brain, can regenerate in some lower vertebrates, they have no capacity for regeneration in the mammalian retina *(2)*. Cell transplantation has been proposed as a potential solution to replace RGCs lost in advanced retinal disease, but poor cell survival rates post-transplantation have limited the effectiveness and further development of this strategy *(3–6)*.

The glaucomatous retina is typically characterized by increased interocular pressure (IOP), which can cause inflammation, immune cell infiltration, and host cell reactivity *(7, 8)*. Even after the IOP normalizes this, a toxic microenvironment can persist *(8)*, making it challenging for transplanted donor cells to survive in the host retina. Further, after transplantation, donor cells encounter an environment that lacks adequate oxygenation

and metabolic support until they structurally integrate into their respective positions within the host retina. This deficiency can intensify the stress experienced by the donor cells, leading to further decreased survival rates. To overcome these limitations and establish a more favorable microenvironment, we identified and delivered pro-survival factors into the retina to improve donor RGC survival after transplantation.

Here, by analyzing the single-cell transcriptome of the developing human retina (FD59, FD82, FD125), we identified brain-derived neurotrophic factor (BDNF) and glial-derived neurotrophic factor (GDNF) as being highly expressed during development but no longer present during adulthood. Through this in silico analysis, we further demonstrate that BDNF and GDNF are necessary to prevent apoptosis and host RGCs are the primary source of endogenous BDNF in the retina, suggesting that supplementing transplants with exogenous neurotrophic factors may improve donor RGC survival in an RGC-depleted retina.

In this report, we show that slow-release BDNF and GDNF can improve the RGC differentiation yield and survival in retinal organoids in vitro. Further, we confirm that co-delivery of mouse and human stem cell-derived RGCs with slow-release formulations of BDNF and GDNF improves donor RGC coverage within the retina and the total number of cells that survive post-transplantation. Lastly, we demonstrate that a slow-release formulation of BDNF and GDNF provides a neuroprotective effect on host RGC, preventing a decrease in electroretinogram-related response caused by glutamate-induced neurotoxicity.

Methods:

Mouse Stem Cell-derived RGC Differentiation

Induced pluripotent stem cells (iPSCs) derived from Tg[Thy1.2-Green Fluorescent Protein (GFP)]M mice were cultured on gelatin-coated (0.2% v/v) flasks in standard culture conditions (37°C, >95% humidity, 5% CO2). Mouse stem cell maintenance medium [10% fetal bovine serum (FBS), 1x L-glutamine, 1x non-essential amino acids, 1x sodium pyruvate, 1x antibiotic-antimycotic, 1x EmbryoMax Nucleosides, 100 μM β-Mercaptoethanol, and 100 U/mL mouse leukemia inhibitory factor in DMEM/F12 (3500 mg/L dextrose)] was replaced every two days until the iPSC colonies approached approximately 70% confluency. Upon reaching 70% confluency, iPSCs were harvested using 1x trypsin-EDTA and either transferred to new gelatin-coated flasks at a density of 2000 cells/cm² or used for retinal ganglion cell (RGC) differentiation as previously detailed. For RGC differentiation, 1500 cells were initially seeded in 50 μL of Optic Vesicle (OV) medium [1x L-glutamine, 1x non-essential amino acids, 1x sodium pyruvate, 1x antibiotic-antimycotic, 1x lipid concentrate, 0.2x Insulin-Transferrin-Selenium-Ethanolamine, 100 μM β-Mercaptoethanol, 1.5% FBS, 1 μM N-Acetyl-L-cysteine (NAC), and 10 μM forskolin in DMEM/F12 (3500 mg/L dextrose)] per well in uncoated 96-well U-bottom polystyrene plates. After 24 hours in standard culture conditions, each well received an additional 50 μL of OV medium with 2% Matrigel to start forebrain/retinal differentiation. The next day, 100 μL of OV medium with 1% Matrigel was added to each well. The organoids were then maintained in this medium until the ninth day of differentiation, with half of the medium being replaced every two days. On day 9, the organoids were extracted from the plates, randomly sectioned to isolate optic vesicles for expanded growth, and transferred to low-attachment flasks. From this point, they were

kept in Optic Cup (OC) medium [1x L-glutamine, 1x non-essential amino acids, 1x sodium pyruvate, 1x antibiotic-antimycotic, 1x lipid concentrate, 100 μM β-Mercaptoethanol, 1x B27 without vitamin A, 1 μM N-Acetyl-L-cysteine (NAC), and 10 μM forskolin in DMEM/F12 (3500 mg/L dextrose)]. Half the medium was replaced every other day from day 21 to 25 of retinal maturation. Starting from day 16, the OC medium was further supplemented with 250nM all-trans-retinoic acid.

Human Stem Cell-derived RGC Differentiation

Colonies of H9-BRN3B:tdTomatoThy1.2-hESCs were cultured on six-well plates coated with 2% Matrigel with mTeSR1 media in a low oxygen incubator (5% CO2, 3.5% O2, above 95% humidity, 37°C). Media was replaced daily. When the cell density reached around 70% after 4-5 days, the cells were detached using accutase for 8 minutes at room temperature and transferred to a new Matrigel-coated plate at a ratio between 1:10 and 1:20.

Human RGCs were differentiated in 3D retinal organoid cultures as previously described. During cell passaging, hESC colonies were enzymatically dissociated for 12 minutes to form a single-cell suspension. To create embryoid bodies, 7,500 hESCs per well were seeded in an ultra-low attachment 96-well U-bottom plate in a low oxygen incubator for 24 hours. After 24 hours, the plate was moved to standard culture conditions. The differentiation media was exchanged daily and transitioned from a 3:1 mix of mTeSR1 and BE6.2-NIM [B27 + E6 at 2X concentration – neural induction medium: 1x L-glutamine, 1x sodium pyruvate, 1x antibiotic-antimycotic, 1x B27 without Vitamin A, 0.88 mg/mL NaCl, 38.8 mg/L insulin, 128 mg/L L-ascorbic acid, 28 μg/L selenium, 21.4 mg/L

transferrin, and 38.8 mg/L $NaHCO_3$ in DMEM/F12 (3500 mg/L dextrose)] to primarily BE6.2-NIM by day 8. To support neural and early retinal development, the media was supplemented with 20 μM Y-27632 on day 0, 1% Matrigel from days 2 to 6, 3μM IWR-1-endo from days 1 to 4, and 55 ng/mL BMP4 on day 6. On day 8, organoids were randomly sectioned to isolate optic vesicles, facilitating growth and keeping size under the diffusion limit (1.4 mm in diameter). These chopped organoids were then placed on tissue culture-treated plastic in Long-Term Retinal Differentiation Media (LT-RDM) [1x L-glutamine, 1x sodium pyruvate, 1x antibiotic-antimycotic, 1x B27, 1x non-essential amino acids, and 10% FBS in 50:50 1x DMEM/F12 (3500 mg/L Dextrose):DMEM (4500 mg/mL dextrose)] to encourage attachment and retinal epithelium growth. The media was replaced every two days, transitioning to a 1:1 mix of LT-RDM and Retinal Differentiation Media (RDM) [LT-RDM without FBS] by day 17, with added 100nM smoothened agonist (SAG) from days 12 to 16. On day 17, the retinal tissue clusters were detached and moved to a poly(2-hydroxyethyl methacrylate)-coated flask for suspension culture in RDM supplemented with 100nM SAG. From day 18 onwards, the media, now a 1:3 mix of LT-RDM and RDM with 2.5% FBS and 100nM SAG, was replaced every other day, gradually transitioning to pure LT-RDM by day 24. From day 26, the media was further supplemented with 1mM taurine, and from day 32, 250nM all-trans-retinoic acid. The LT-RDM was replaced every other day until retinal organoids were collected for dissociation.

RGC Isolation

To dissociate mature mouse (d21) and human retinal organoids (d44 – 48), the embryoid body dissociation kit from Miltenyi Biotec (catalog number 130-096-348) was used with

the gentleMACS™ Dissociator, following the instructions provided by the manufacturer, with a single adjustment. The preset gentleMACS programs EB_01 and EB_02 were substituted with Brain_01 and Brain_02, respectively. After dissociation, mouse and human RGCs (Thy1.2-positive cells) were isolated by magnetic microbead-based sorting using the Dynabeads™ FlowComp™ Mouse Pan T (CD90.2) Kit from Invitrogen (catalog number 11465D), following the manufacturer's instructions.

Single-cell RNA Sequencing Data Analysis

Single-cell RNA sequencing data analysis was performed in RStudio v. 2022.07.2 (R language v. 4.2.1) using previously published datasets from the human fetal retina (FD59, FD82, FD105) *(9)*. Raw data was processed as previously described *(10)*. For the stages FD82 and FD105, the analysis included both the peripheral and central retina. Seurat objects with annotated UMAP embeddings are available in the source data file.

To show the changes of gene expression for different timepoints, the AverageExpression function in Seurat was applied to the whole datasets. Trends for GDNF and BDNF average expression at different time points plots were visualized using ggplot2 (v. 3.3.6) and ggalt (v. 0.4.0) packages *(11)*.

The analysis also included a step with correlation between NTRK2, GDNF receptor, and GFRA1, GDNF receptor and apoptosis pathway genes expression. To obtain the gene list for apoptosis, we downloaded the annotation from Molecular Signatures Database (http://www.gsea-msigdb.org/gsea/msigdb/human/geneset/HALLMARK_APOPTOSIS.html).

To check the apoptosis pathway expression, we used the escape package (v. 1.6.0) *(12)*. We merged subsetted RGCs populations in FD59, FD82, and FD125 Seurat objects and performed the enrichment on the RNA count data using the enrichIt function with the ssGSEA method *(13)*. To examine the correlation between NTRK2/GFRA1 and the apoptosis pathway expression, we generated a plot using FeatureScatter Seurat function for the GFRA1 positive and NTRK2 positive cells. We added regression model to the analysis using geom_smooth function with 'lm' method.

To obtain the information related to incoming and outgoing cluster ligand-receptors interactions, we used the CellChat package (v. 1.5.0) for FD59, FD82, and FD125 timepoints using our Seurat objects as previously described *(14)*. To avoid the projection reducing the dropout effects of signaling genes, in particular for possible zero expression of subunits of ligands/receptors, we used raw.use = FALSE setting in computeCommunProb function. We also used population.size = TRUE parameter to consider the effect of cell proportion in each cell group in the probability calculation. Please contact the corresponding author for CellChat files in .rds format.

The software and packages used for the analysis can be found in Table S1. The code used for this study to reproduce the bioinformatical analysis is available on GitHub at https://github.com/mcrewcow/BaranovLab/blob/main/survival_RGC_paper.R.

<u>Donor RGC Transplantation</u>

Donor RGC transplantations were performed at the Schepens Eye Research Institute of Mass. Eye and Ear following the Institutional Animal Care and Use Committee (IACUC)

and Association for Research in Vision and Ophthalmology (ARVO) guidelines. To support donor RGCs and establish a proneuronal microenvironment, we formulated our mouse or human donor RGCs with selected pro-survival factors. To avoid repeated intraocular injections, which could cause additional inflammation and reduce donor RGC viability, we formulated donor RGCs with slow-release neurotropic factors (GDNF- and BDNF-loaded polyhedrin-based particles (PODS)). Donor RGCs were transplanted (10,000 – 20,000 RGCs/retina) into adult (1- to 4-month-old) RGC-deficient mouse retinas (inherited loss or neurotoxic model) with and without PODS under a general (ketamine/xylazine intraperitoneal injections) and local (0.5% proparacaine eye drops) anesthetic. Donor RGC suspensions (1 μL) were injected intravitreally using a beveled glass microneedle with an inner diameter of 80 μm at a flow rate of 1 μL per minute. Mice were kept on a standard 12-hour light-dark cycle and were euthanized at predetermined endpoints—2 weeks for transplants from the same species (syngeneic) and 3 days for cross-species (xenotransplantation) transplants—using CO2 inhalation. Three to fourteen days after transplantation, eyes were enucleated, fixed for 24 hours at room temperature in 4% paraformaldehyde, and then processed for retinal flat-mount preparation. Retinas were stained for host and donor cells to assess RGC survival and neurites (8 – 11 mice/group). Specifically, eyes were enucleated after three days for human donor RGC transplants to minimize immune reactions typical of xenotransplantation and after fourteen days for mouse donor RGCs to allow for neurite outgrowth.

<u>Electroretinogram</u>

To measure functional recovery following transplantation, mice were injected with NMDA 1 week prior to intravitreal injection of donor RGCs to cause RGC death and subsequently received either cells alone, cells+PODS, or PODS alone. Electroretinography (ERG) was performed at 6 weeks post-transplant to assess host retinal function. Before recording electrical activity in the retina with ERG, mice were dark-adapted overnight. Mice were then anesthetized with ketamine (120 mg/kg) and xylazine (20 mg/kg), administered intraperitoneally with a 25G needle. The pupils of each mouse were dilated using 1% Tropicamide, followed by the application of Genteal to maintain corneal moisture. Mice were positioned on a temperature-controlled platform on the ERG machine (Diagnosys LLC). Reference and ground electrodes were placed under the skin on the forehead and tail, respectively. Two gold-ring electrodes were carefully positioned on the corneas without blocking the pupil. A drop of artificial tear solution was applied to ensure hydration throughout the experiment. The positive scotopic threshold response (pSTR) data were gathered using a series of flashes, with an average of 40 responses for each intensity level. The pSTR was quantified by measuring the amplitude from the baseline to the peak of the positive wave. Post-ERG, the eyes were treated with antibiotic ointment and artificial tears. The mice were then placed on a warming pad with a circulation of heated water to stabilize their body temperature, allowing for a safe recovery.

Flow Cytometry

Dissociated cells were resuspended in Cytofix/Cytoperm buffer (BD Biosciences) and fixed. The fixation process involved a 30-minute incubation on ice. Post-fixation, cells were washed using a buffer solution composed of 0.1% Tween 20 and 0.1% Triton-X in

1× PBS and centrifuged at 300 x g for 5 minutes. The cell pellet was resuspended in blocking buffer (10% goat serum, 1% Bovine Serum Albumin (BSA), 0.1% sodium citrate, 0.1% Tween 20, and 0.1% Triton-X in 1× PBS) for 30 minutes at room temperature. Following the blocking, the cells underwent another cycle of washing and centrifugation under the same conditions as previously mentioned. For staining, the cells were first resuspended in a staining buffer (1% BSA, 0.1% Tween 20, and 0.1% Triton-X in 1× PBS). Primary antibodies were added to the cells overnight at 4°C on an orbital shaker. Post-primary antibody incubation, the cells were washed and centrifuged again. Secondary antibodies were then added to the cells for 3-hour incubation at room temperature. The cells underwent a final set of washes and centrifugations. After the last washing step, cells were resuspended in the staining buffer in preparation for flow cytometric analysis. The samples were analyzed using a BD LSR II flow cytometer. Data acquisition and gating were performed using FlowJo software. The gating strategy involved selecting single cells based on forward/side scatter and a nuclear marker. This approach was designed to exclude both small particulate debris and multi-cell aggregates from the analysis. Isotype controls were employed to correct for background fluorescence in the final target gates.

Immunohistochemistry

To visualize RGCs in culture, organoids, retinal flat-mounts, and retinal sections, samples were fixed for 30 min for cell culture and >4 hours for tissue samples with 4% (v/v) paraformaldehyde at room temperature. For retinal sections, eyes were sent to the Schepens Eye Research Institute Morphology Core for paraffin embedding (producing 6

μm thick sections) and Hematoxylin and Eosin (H&E) staining. The paraffin-embedded sections were first treated with an xylene substitute, followed by a series of ethanol washes. Antigen retrieval was then performed using a sodium citrate buffer (10 mM Sodium citrate, 0.05% Tween-20, pH 6.0) for 30 minutes.

For immunofluorescence staining, samples were incubated overnight (>12 hours) at 4°C with 1:400 goat anti-mouse secondary antibody in blocking buffer (10% goat serum, 1% bovine serum albumin, 0.1% sodium citrate, 0.25% Tween-20, 0.25% Triton-X, and 0.3M glycine in 1x phosphate-buffered saline) to reduce non-specific staining. Following blocking, the RGCs and retinal tissues were incubated with primary antibodies in staining buffer (1% bovine serum albumin, 0.25% Tween-20, and 0.25% Triton-X in 1x PBS) for 48 to 72 hours at 4°C. A full list of primary antibodies and their concentrations is provided in Table S2. Post-primary antibody incubation, tissues were washed three times in wash buffer (0.1% Tween-20, 0.1% Triton-X in 1x PBS) to remove unbound antibodies. Secondary antibodies (goat anti-chicken, goat anti-rabbit, and goat anti-mouse) were then added at a 1:500 dilution in staining buffer and incubated for 12 to 24 hours at 4°C. Following another triple wash, the samples were stained with 1 μg/mL DAPI in PBS for 20 minutes to highlight cell nuclei. To reduce tissue autofluorescence, samples were treated with 10 mM copper sulfate (pH 5.0) at room temperature for 15 minutes. After a final PBS rinse, the samples were mounted between glass cover slides and coverslips using a polyvinyl alcohol-based mounting medium containing an antifade agent (1,4-Diazabicyclo[2.2.2]octane). Imaging was performed using an Olympus IX83-FV3000 confocal microscope.

Enzyme-linked immunosorbent assay (ELISA)

BDNF ELISA (Boster #EK0307) was performed according to the manufacturer's protocol. PBS solution (50 µl) containing either 1e6, 5e5, 2e5, 5e4, or 1e4 PODS® BDNF were added to wells of a 96-well plate and were spun down at 3000 g for 25 min. PBS was removed, and the plate was dried in a laminar flow cabinet. RPMI 1640 Complete Medium supplemented with 10% bovine calf serum was added to each well (100 µl/well). The plate was then incubated at 37 °C, 5% CO2. For the release time curve, medium from wells with 1e6 PODS® was collected on days 1, 2, 3, 4, and 7 after medium addition and stored at -20 °C. For the dose-response curve, the medium was collected on day 4 after medium addition.

Results:

BDNF and GDNF are Key Neurotrophic Factors in Retinal Development and RGC Survival

We performed an in silico analysis of the single-cell transcriptome of developing human retinas across various developmental stages (FD59, FD82, FD125) to determine which molecular features were present during development but not during adulthood. Specifically, we evaluated changes in gene expression of every previously identified neurotropic factor over time and identified Brain-Derived Neurotrophic Factor (BDNF) and Glial Cell-Derived Neurotrophic Factor (GDNF) as genes of interest that fit this profile. Both these factors were prominently expressed during the early stages of retinal development, particularly in phases where RGCs undergo differentiation and maturation

(**Figure 1A**). However, their levels markedly diminish as the retina matures, indicating we may need to supplement the retina with these proneuronal factors to reestablish an environment to support RGC repopulation.

Furthermore, by examining the relationship between BDNF/GDNF expression and apoptosis pathway genes, we found a clear negative correlation (**Figure 1B**), indicating that higher levels of BDNF and GDNF are associated with reduced activation of cell death pathways. This relationship underscores the potential of these neurotrophic factors in promoting RGC survival, especially in conditions where these cells are at risk, such as in glaucoma.

we then analyzed ligand-receptor interactions to understand the communication pathways involving BDNF and GDNF using CellChat *(14)*. This analysis provided insights into how these factors signal within the retinal environment, distinguishing between autocrine signaling, where cells respond to the signals they emit, and paracrine signaling, involving communication between different cell types. Since our analysis shows that RGCs are the primary source of BDNF and GDNF in the retina (**Figure 1C**), their loss in diseases like glaucoma creates an environment lacking these crucial survival factors. Supplementing transplanted cells with BDNF and GDNF could, therefore, not only enhance the survival of these cells but also potentially rejuvenate the surrounding retinal tissue, creating a more favorable environment for transplantation, regeneration, and repair.

BDNF and GDNF Treatment Enhances RGC Differentiation and Survival *In Vitro*

Growth factors have been widely described for aiding in the survival and differentiation of neurons in vitro *(15)*. Classified into 40 subtypes by morphology, differential gene expression, and functional diversity, RGCs are integral to functional vision *(16–19)*. While the biological significance of RGC diversity is not understood, it is essential to consider when assessing donor cell populations for cell replacement. Here, we utilize a slow-release formation of BDNF and GDNF (BDNF and GDNF-loaded polyhedrin-based particles (PODS)) to investigate the role of these neurotropic factors in RGC differentiation and subtype specification. BDNF and GDNF-loaded PODS show approximately 50 pg/mL sustained growth factor release in culture over a full week (**Figure S1**). The inclusion of BDNF and GDNF PODS in our mouse RGC differentiation resulted in a 46% increase in RBPMS+ RGC population within late-stage (D30) cultures as compared to non-treated controls (**Figure 2**). Amongst others, organoid-derived RGCs expressed markers including Spp1, Kcng4/Osteopontin (α-RGCs), and Melanopsin (intrinsically photosensitive RGCs), representing all major RGC subclasses in-vivo *(20)*, within 30 days of culture and are upregulated with PODS co-treatment (**Figure 2**). Moreover, mouse stem cell-derived RGCs were shown to be functional by Ca2+ imaging, and human donor RGC action potentials were recorded using an MEA (**Figure S2**).

Modifying the Retinal Microenvironment with Slow-release BDNF and GDNF Improves RGC Transplantation Outcomes

To mimic RGC loss in glaucoma, we utilized two RGC loss models for transplantation, NMDA-induced toxicity and an inherited loss model (**Figure S3**). Our transplantation experiments in these mice demonstrated that delivering BDNF/GDNF-PODS with human

and mouse donor RGCs significantly improved the transplantation outcome. The success rate of mouse donor RGC transplantations, defined as a transplant with more than 0.5% of delivered donor RGCs surviving *(5)*, increased to 73% from 37% with the co-treatment of BDNF/GDNF-PODS. Moreover, the PODS formulation led to a 2.7-fold increase in donor mouse RGC coverage across the retina, with several neurites extending toward the optic nerve head (**Figure 3**). This finding is critical as it demonstrates that the transplanted cells have the potential to connect with their postsynaptic targets in the brain, a necessary step for functional recovery after injury.

Although the PODS co-treatment did not affect the success rate of human donor RGC transplantation, the PODS formulation led to a 15-fold increase in the total number of human donor RGCs detected in the mouse retina (**Figure 4A-C**). Additionally, 50% of all transplants containing PODS showed donor RGC neurites extending toward the optic nerve head, with an average length of 1008.44 ± 264.12 μm compared to 10% in the control group (**Figure 4D-E**). Critically, these results demonstrate the potential of PODS to improve the survival and integration of transplanted human RGCs, which could lead to functional recovery in patients with retinal degeneration. Donor RGC axon outgrowth and morphology, including entry into the optic nerve head, was enhanced by PODS co-treatment, proposing a benefit of co-treatment for cell delivery.

Delivery of Slow-Release BDNF and GDNF Preserves Host RGC Function after an Induced Optic Neuropathy

To measure retinal function after transplantation, we measure the positive scotopic threshold response using electroretinography to evaluate RGCs *(21, 22)*. Our results

indicate that Thy1-GFP+ donor RGCs alone don't rescue retinal function as assessed by ERG at 6 weeks post-transplantation in the NMDA model of toxic optic neuropathy (**Figure 5**). However, treatment with PODS and cells+PODS led to the partial preservation of RGC function as measured by pSTR response at 6 weeks (32uV in the PODS group vs. 17uV in the control, **Figure 5**), indicating that PODS may provide a neuroprotective effect on host RGCs.

Discussion:

Blindness and vision impairments resulting from the loss or degeneration of retinal ganglion cells (RGCs) are irreversible. While the underlying pathology of optic neuropathies (ON) is diverse (e.g., elevation of intraocular pressure, acute trauma), all phenotypically resemble neurodegenerative disease. From an initial decrease in the visual field, congruent with dyschromatopsia and changes in the pupillary response, patients gradually progress toward a complete loss of vision. Optical coherence tomography and other live imaging approaches have shown that the RGC death in glaucoma is a slow process, thus it is possible to preserve the remaining function and, potentially, reverse some of the vision loss with timely application of pro-survival factors.

Several pro-survival and anti-apoptotic pathways have been utilized as therapeutic targets in glaucoma, including ERk, p38, PTEN, JNK, and others *(23)*. Growth factors like Brain-Derived Neurotrophic Factor (BDNF) and Glial Cell-Derived Neurotrophic Factor (GDNF) have shown significant neuroprotective properties in vitro and in vivo *(24, 25)*. However, a major limitation in the application of each of these factors is their rapid

clearance and low bioavailability at the target site within the eye, necessitating frequent injections. Moreover, once RGCs are lost, these factors alone cannot restore them.

The advent of stem cell technologies has opened new avenues for cell replacement therapies. For instance, in ophthalmology, the first clinical trials and multiple prior research studies have shown the potential of both retinal pigment epithelium (RPE) and photoreceptor replacement to halt visual decline within patients affected by Age-related macular degeneration (AMD) and cone/rod dystrophies *(26, 27)*. Like AMD, glaucoma is a progressive neurodegenerative disease for which cell replacement promises to prevent or recover vision loss *(6)*. However, while uniform cell populations like the RPE may be easy to differentiate in vitro, glaucoma affects a highly diverse class of neurons - RGCs. Furthermore, RGC replacement is further challenged by the need for donor neurons to integrate into the host retina and extend their axons toward the optic nerve head and into the brain.

Nevertheless, RGC replacement by transplantation of either primary or stem cell-derived RGCs is a potential approach to enable vision recovery within advanced-stage optic neuropathies. Our previous work showed that post-transplantation, more than 50% of healthy and even RGC-depleted recipient retinas retained donor RGCs post-transplant. However, the actual number of surviving donor RGCs and retinal area covered by the transplant remained low. To address this challenge, we use BDNF and GDNF as co-treatments to support the survival of both host and donor cells within the diseased microenvironment.

To avoid repeat injections, we utilize polyhedrin-based particles (PODS) for the slow-release co-treatment of BDNF and GDNF. This approach increases not only the number

of donor RGC but also the number of neurites extending into the optic nerve head. These findings are indicative of a potential rewiring of the retina-to-brain connection, a critical step for functional recovery.

The modulation of the host retinal microenvironment through slow-release growth factor treatment represents an innovative and effective approach to improving transplantation outcomes. Furthermore, by enhancing donor RGC morphology and axon outgrowth, this strategy opens up new possibilities in the field of regenerative medicine for the treatment of glaucoma and other optic neuropathies. Using neuroprotective factors in combination with other approaches to modify the retinal microenvironment and stem cell-derived RGC delivery may offer a viable solution to the challenge of RGC replacement. Depending on the model or state of the disease, the retinal microenvironment may also need to be altered to support donor RGC migration, growth, maturation, axon extension, and increased metabolic demands *(10)*. Therefore, the integration of neuroprotective strategies with cell replacement therapies is likely to be a pivotal direction for research and clinical applications. Lastly, slow-release growth factors represent a promising neuroprotective approach to limit RGC death before loss. Altogether, these findings provide promising insights into potential strategies for restoring vision lost due to RGC damage or loss in ONs.

Funding

NIH/NEI–F32EY033211 (J.R.S.), NIH/NEI–L70EY034355 (J.R.S.), NIH/NEI–T32EY007145 (MBED fellowship, J.R.S.), NIH/NEI–5U24EY029893-03 (P.B.), NIH/NEI–P30EY003790 (Core Facility Grant), Bright Focus Foundation–G2020231 (P.B.), NIH/NEI R01EY021482 (T.A.R.), Gilbert Family Foundation–GFF00 (P.B.)

Author contributions:

J.R.S., E.K., J.O., J.M., C.P., and P.B. performed the research; J.R.S. and E.K. analyzed the data; J.R.S. wrote the paper; and P.B. supervised the research.

Competing interests:

Chris Pernstich is an employee at Cell Guidance Systems.

References:

1. Y.-C. Tham, X. Li, T. Y. Wong, H. A. Quigley, T. Aung, C.-Y. Cheng, Global Prevalence of Glaucoma and Projections of Glaucoma Burden through 2040 A Systematic Review and Meta-Analysis. *Ophthalmology* **121**, 2081–2090 (2014).

2. L. Erskine, E. Herrera, Connecting the Retina to the Brain. *Asn Neuro* **6**, 1759091414562107 (2014).

3. K. Y. Zhang, E. A. Aguzzi, T. V. Johnson, Retinal Ganglion Cell Transplantation: Approaches for Overcoming Challenges to Functional Integration. *Cells* **10**, 1426 (2021).

4. P. Venugopalan, Y. Wang, T. Nguyen, A. Huang, K. J. Muller, J. L. Goldberg, Transplanted neurons integrate into adult retinas and respond to light. *Nat Commun* **7**, 10472 (2016).

5. J. Oswald, E. Kegeles, T. Minelli, P. Volchkov, P. Baranov, Transplantation of miPSC/mESC-derived retinal ganglion cells into healthy and glaucomatous retinas. *Mol Ther - Methods Clin Dev* **21**, 180–198 (2021).

6. J. R. Soucy, E. A. Aguzzi, J. Cho, M. J. Gilhooley, C. Keuthan, Z. Luo, A. Monavarfeshani, M. A. Saleem, X.-W. Wang, J. Wohlschlegel, T. Rr. Consortium, P. Baranov, A. D. Polo, B. Fortune, K. K. Gokoffski, J. L. Goldberg, W. Guido, A. L. Kolodkin, C. A. Mason, Y. Ou, T. A. Reh, A. G. Ross, B. C. Samuels, D. Welsbie, D. J. Zack, T. V. Johnson, Retinal ganglion cell repopulation for vision restoration in optic neuropathy: a roadmap from the RReSTORe Consortium. *Mol. Neurodegener.* **18**, 64 (2023).

7. L. Storgaard, T. L. Tran, J. C. Freiberg, A. S. Hauser, M. Kolko, Glaucoma Clinical Research: Trends in Treatment Strategies and Drug Development. *Frontiers Medicine* **8**, 733080 (2021).

8. S. Tehrani, L. Davis, W. O. Cepurna, T. E. Choe, D. C. Lozano, A. Monfared, L. Cooper, J. Cheng, E. C. Johnson, J. C. Morrison, Astrocyte Structural and Molecular Response to Elevated Intraocular Pressure Occurs Rapidly and Precedes Axonal Tubulin Rearrangement within the Optic Nerve Head in a Rat Model. *Plos One* **11**, e0167364 (2016).

9. A. Sridhar, A. Hoshino, C. R. Finkbeiner, A. Chitsazan, L. Dai, A. K. Haugan, K. M. Eschenbacher, D. L. Jackson, C. Trapnell, O. Bermingham-McDonogh, I. Glass, T. A. Reh, Single-Cell Transcriptomic Comparison of Human Fetal Retina, hPSC-Derived Retinal Organoids, and Long-Term Retinal Cultures. *Cell Reports* **30**, 1644-1659.e4 (2020).

10. J. R. Soucy, L. Todd, E. Kriukov, M. Phay, V. V. Malechka, J. D. Rivera, T. A. Reh, P. Baranov, Controlling donor and newborn neuron migration and maturation in the eye through microenvironment engineering. *Proc. Natl. Acad. Sci.* **120**, e2302089120 (2023).

11. H. Wickham, ggplot2, Elegant Graphics for Data Analysis. *R* (2016), doi:10.1007/978-3-319-24277-4.

12. N. Borcherding, A. Vishwakarma, A. P. Voigt, A. Bellizzi, J. Kaplan, K. Nepple, A. K. Salem, R. W. Jenkins, Y. Zakharia, W. Zhang, Mapping the immune environment in clear cell renal carcinoma by single-cell genomics. *Commun Biology* **4**, 122 (2021).

13. D. A. Barbie, P. Tamayo, J. S. Boehm, S. Y. Kim, S. E. Moody, I. F. Dunn, A. C. Schinzel, P. Sandy, E. Meylan, C. Scholl, S. Fröhling, E. M. Chan, M. L. Sos, K. Michel,

C. Mermel, S. J. Silver, B. A. Weir, J. H. Reiling, Q. Sheng, P. B. Gupta, R. C. Wadlow, H. Le, S. Hoersch, B. S. Wittner, S. Ramaswamy, D. M. Livingston, D. M. Sabatini, M. Meyerson, R. K. Thomas, E. S. Lander, J. P. Mesirov, D. E. Root, D. G. Gilliland, T. Jacks, W. C. Hahn, Systematic RNA interference reveals that oncogenic KRAS-driven cancers require TBK1. *Nature* **462**, 108–112 (2009).

14. S. Jin, C. F. Guerrero-Juarez, L. Zhang, I. Chang, R. Ramos, C.-H. Kuan, P. Myung, M. V. Plikus, Q. Nie, Inference and analysis of cell-cell communication using CellChat. *Nat Commun* **12**, 1088 (2021).

15. D. Lowenstein, L. Arsenault, The effects of growth factors on the survival and differentiation of cultured dentate gyrus neurons. *J. Neurosci.* **16**, 1759–1769 (1996).

16. T. Baden, P. Berens, K. Franke, M. R. Rosón, M. Bethge, T. Euler, The functional diversity of retinal ganglion cells in the mouse. *Nature* **529**, 345–350 (2016).

17. J. R. Sanes, R. H. Masland, The Types of Retinal Ganglion Cells: Current Status and Implications for Neuronal Classification. *Annu Rev Neurosci* **38**, 1–26 (2015).

18. L. A. Laboissonniere, J. J. Goetz, G. M. Martin, R. Bi, T. J. S. Lund, L. Ellson, M. R. Lynch, B. Mooney, H. Wickham, P. Liu, G. W. Schwartz, J. M. Trimarchi, Molecular signatures of retinal ganglion cells revealed through single cell profiling. *Sci. Rep.* **9**, 15778 (2019).

19. B. A. Rheaume, A. Jereen, M. Bolisetty, M. S. Sajid, Y. Yang, K. Renna, L. Sun, P. Robson, E. F. Trakhtenberg, Single cell transcriptome profiling of retinal ganglion cells identifies cellular subtypes. *Nat Commun* **9**, 2759 (2018).

20. K. B. Langer, S. K. Ohlemacher, M. J. Phillips, C. M. Fligor, P. Jiang, D. M. Gamm, J. S. Meyer, Retinal Ganglion Cell Diversity and Subtype Specification from Human Pluripotent Stem Cells. *Stem Cell Rep.* **10**, 1282–1293 (2018).

21. A. Y. M. Wang, V. H. Y. Wong, P. Y. Lee, B. V. Bui, S. Dudczig, K. A. Vessey, E. L. Fletcher, Retinal ganglion cell dysfunction in mice following acute intraocular pressure is exacerbated by P2X7 receptor knockout. *Sci. Rep.* **11**, 4184 (2021).

22. B. J. Smith, X. Wang, B. C. Chauhan, P. D. Côté, F. Tremblay, Contribution of retinal ganglion cells to the mouse electroretinogram. *Doc Ophthalmol* **128**, 155–168 (2014).

23. A. C. Gauthier, J. Liu, Epigenetics and Signaling Pathways in Glaucoma. *BioMed Res. Int.* **2017**, 5712341 (2017).

24. E. V. Mitroshina, T. A. Mishchenko, O. M. Shirokova, T. A. Astrakhanova, M. M. Loginova, E. A. Epifanova, A. A. Babaev, V. S. Tarabykin, M. V. Vedunova, Intracellular

Neuroprotective Mechanisms in Neuron-Glial Networks Mediated by Glial Cell Line-Derived Neurotrophic Factor. *Oxidative Med. Cell. Longev.* **2019**, 1036907 (2019).

25. E. Palasz, A. Wysocka, A. Gasiorowska, M. Chalimoniuk, W. Niewiadomski, G. Niewiadomska, BDNF as a Promising Therapeutic Agent in Parkinson's Disease. *Int. J. Mol. Sci.* **21**, 1170 (2020).

26. S. R. Grob, A. Finn, T. D. Papakostas, D. Eliott, Clinical Trials in Retinal Dystrophies. *Middle East Afr. J. Ophthalmol.* **23**, 49–59 (2016).

27. V. Klymenko, O. G. G. Martínez, M. Zarbin, Recent Progress in Retinal Pigment Epithelium Cell-Based Therapy for Retinal Disease. *Stem Cells Transl. Med.* , szae004 (2024).

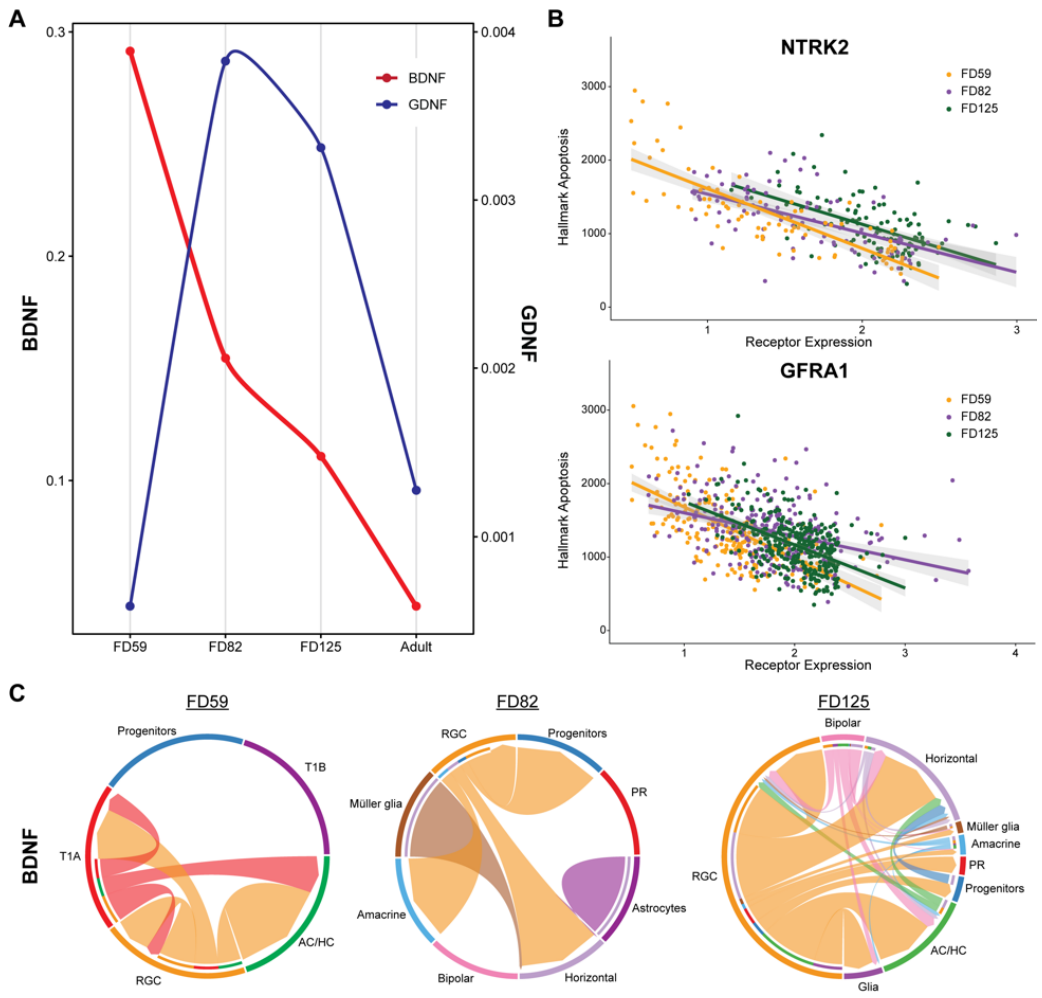

Figure 1. Characterization of neurotropic factors in retinal microenvironment during development. (A) Expression levels of BDNF and GDNF in the retina during different stages of development. **(B)** Correlation between BDNF and GDNF receptor expression and apoptotic genes. **(C)** Chord diagram showing cell-cell communication for the BDNF pathway.

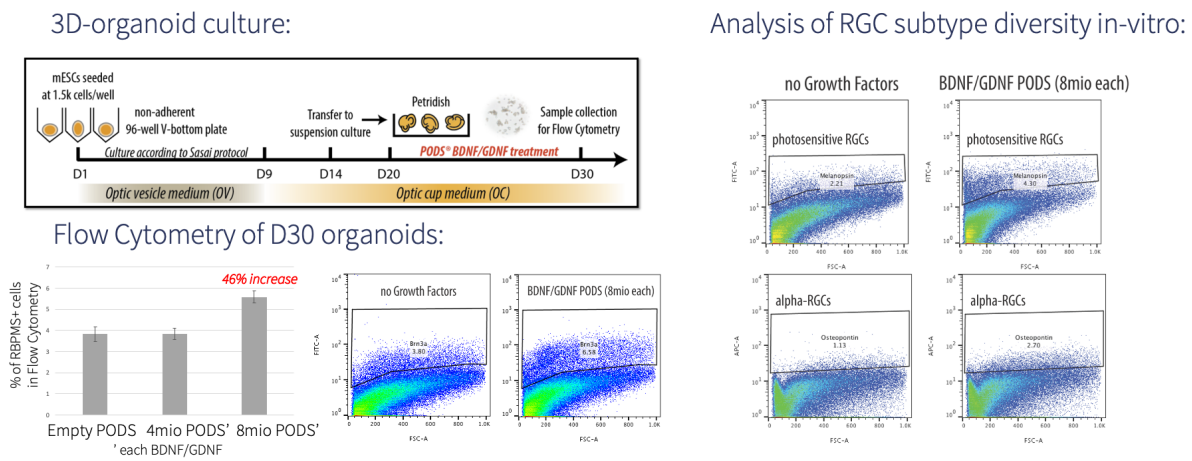

Figure 2. BDNF/GDNF-PODS enhance RGC differentiation yield. PODS co-treatment for 10 days after differentiation improves RGC yield and subtype specification (Melanopsin- and Osteopontin-positive RGCs).

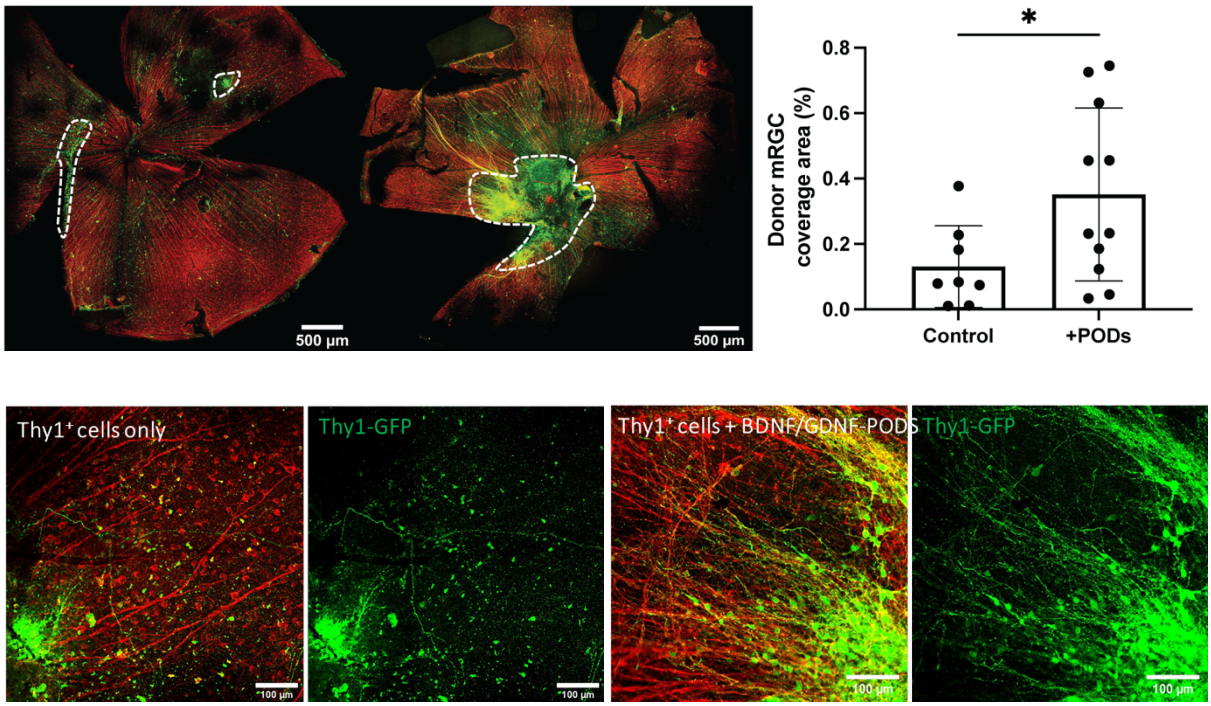

Figure 3. Mouse stem cell-derived RGC syngeneic transplantation in response to BDNF/GDNG co-treatment. Representative retinal whole mount showing mouse donor RGC outgrowth (green) and quantification of coverage area. High magnification images showing mouse donor RGC neurite extensive outgrowth with PODS co-treatment.

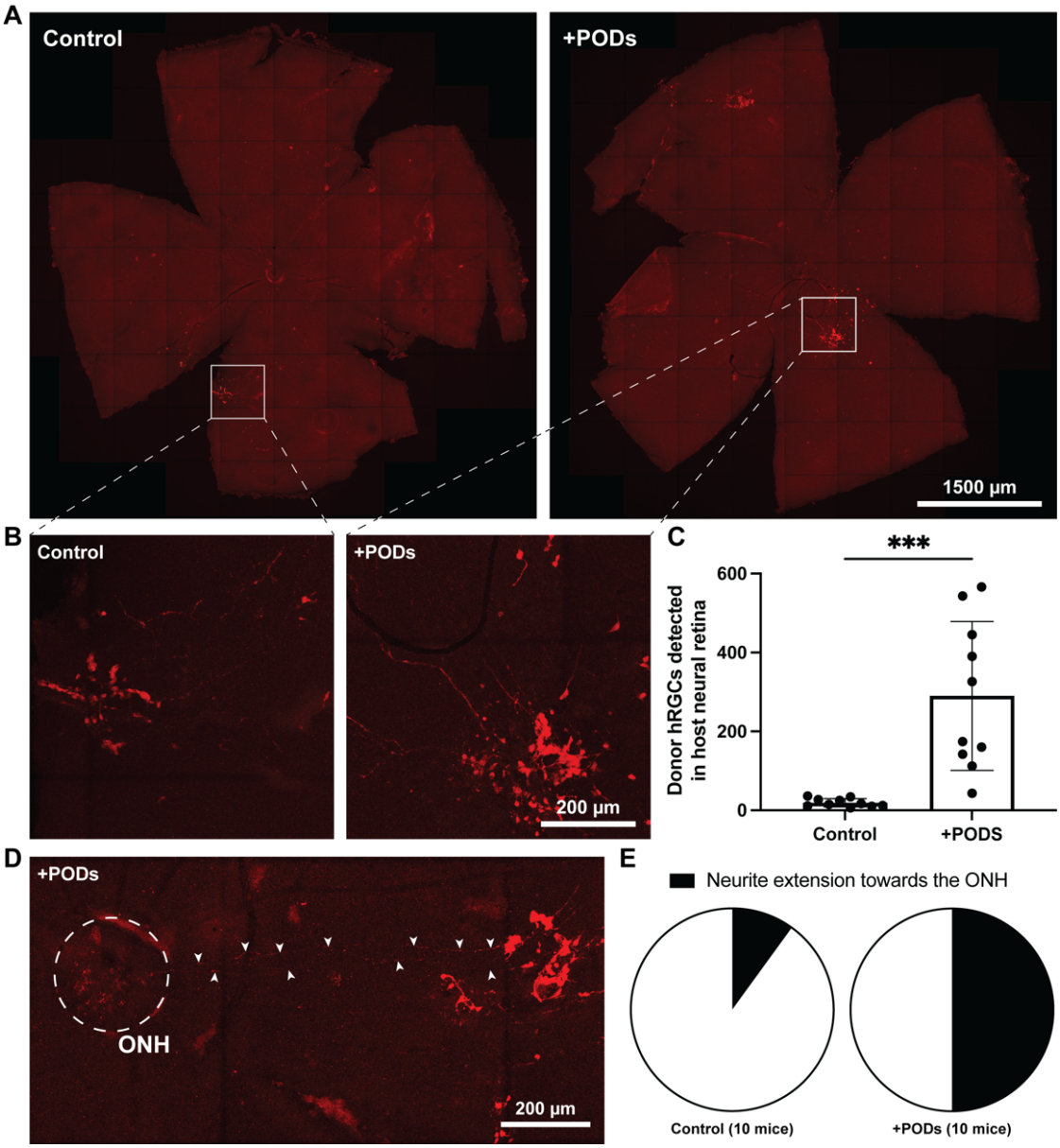

Figure 4. Human stem cell-derived RGC xenotransplantation in mice supplemented with slow-release neurotrophic factors. (A) Representative retinal flat mounts and **(B)** high magnification images showing human donor RGC outgrowth (red) and **(C)** quantification of the number of donor RGCs detected in the host retina for RGCs formulated with and without PODS.

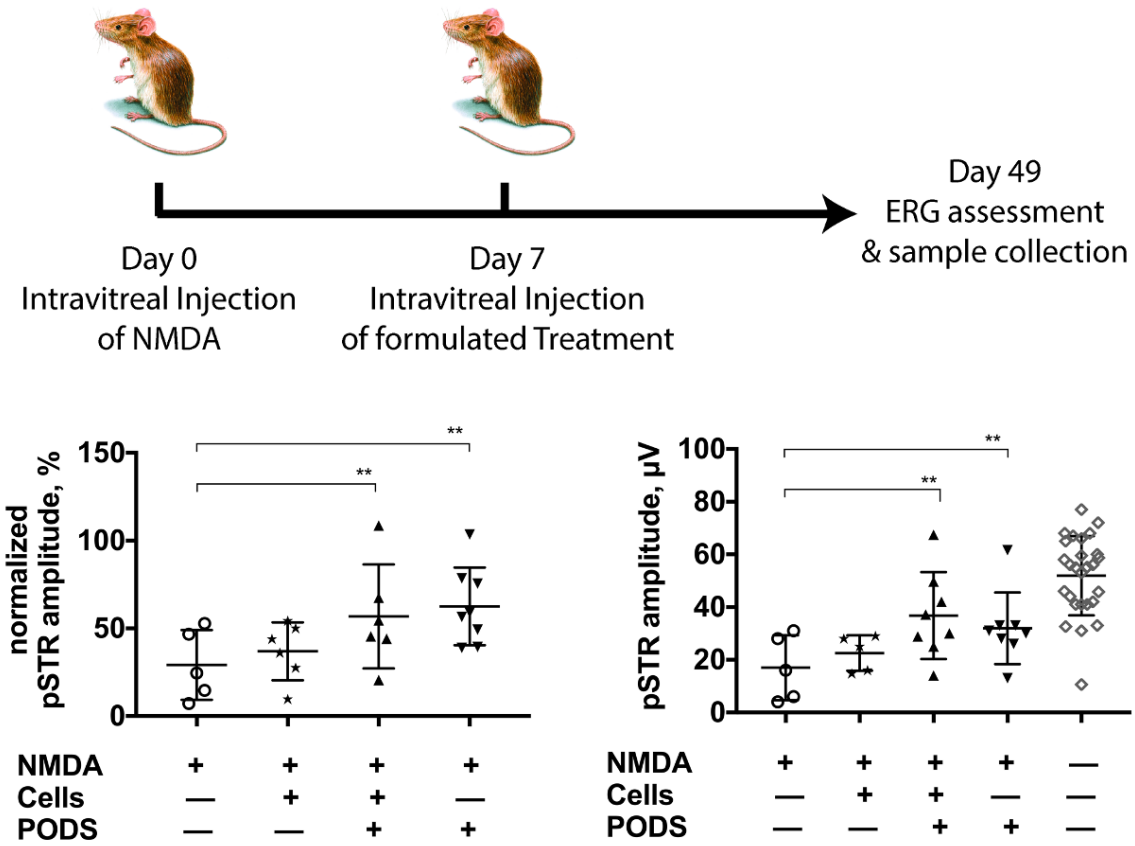

Figure 5. BDNF/GDNF-PODS improve host RGC function in an NMDA-induced toxicity model. Timeline for electroretinogram (ERG) assessment to quantify RGC function in an NMDA-induced toxicity model. Quantification of positive scotopic threshold response (pSTR) measurements after transplantation and BDNF/GDNF-PODS co-treatment.

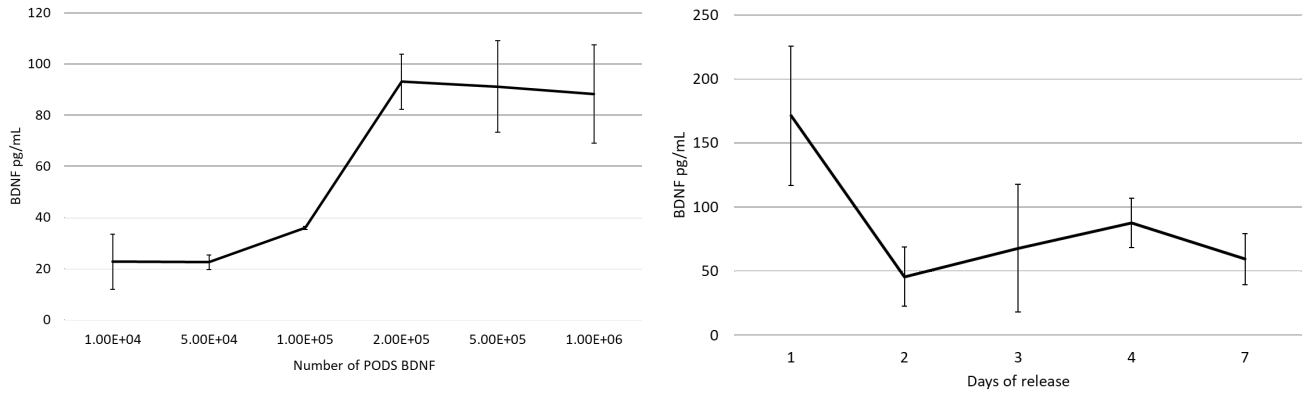

Figure S1. GDNF and BDNF in PODS. The release of BDNF from BDNF-polyhedrin complexes showed both time- and dose-dependence of release.

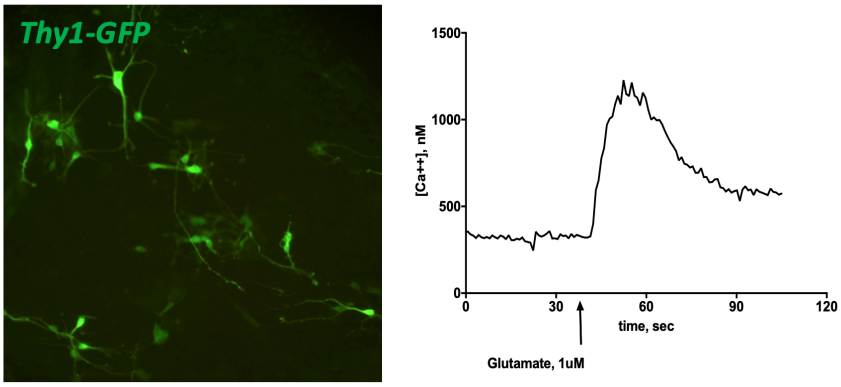

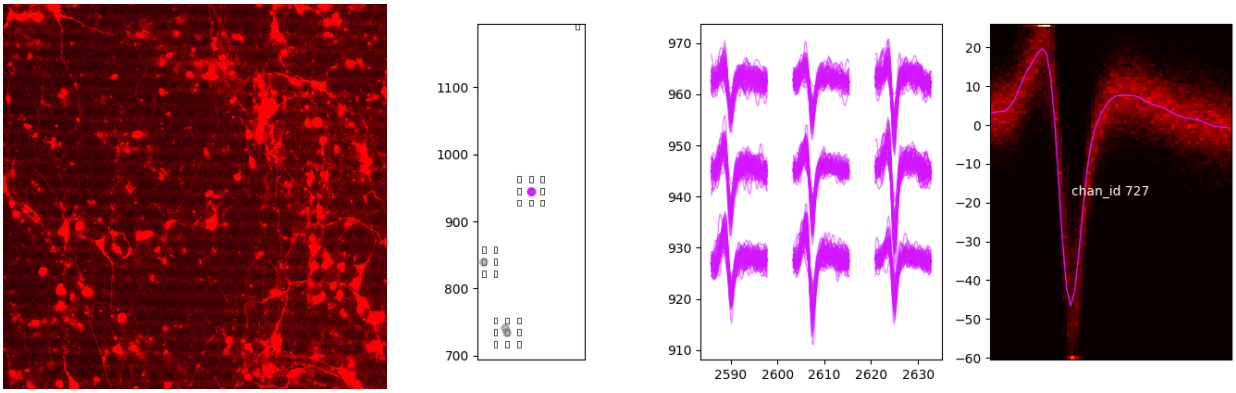

Figure S2. Mouse and human stem cell-derived RGC function. Mouse stem cell-derived RGC function was evaluated using Ca2+ imaging (Fura-2 AM) in response to 1uM Gluatmate. Human stem cell-derived RGC function was evaluated by recording spontaneous action potentials using a multielectrode array after two weeks in culture. Automated spike sorting was used to isolate individual neurons.

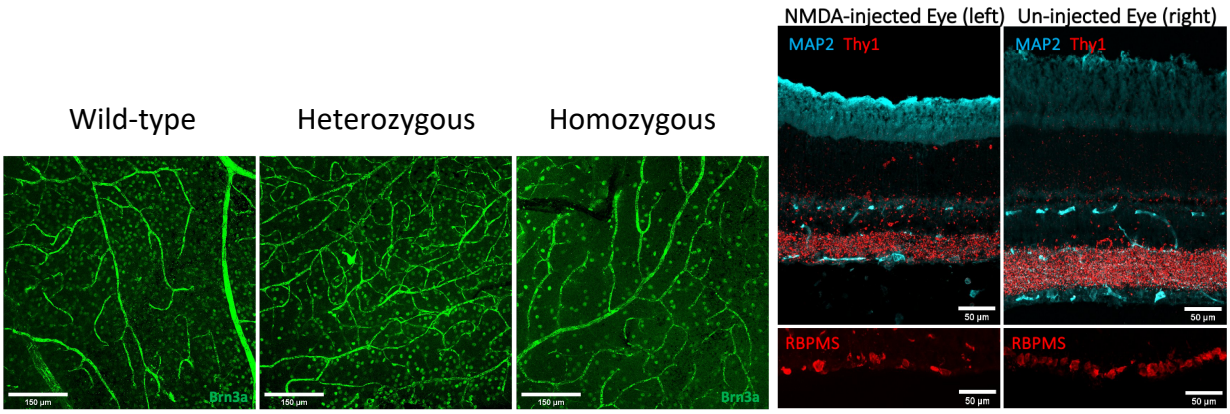

Figure S3. Inherited loss or neurotoxic mouse models. Representative fluorescent images of retinal flat mounts and sections showing RGC loss in an inherited loss model (homozygous) and neurotoxic models (NMDA-injected).

1 **Table S1. Software packages for single-cell RNA sequencing analysis**

Software /package	Version	Link
R	4.2.1	https://cran.r-project.org/bin/
RStudio	2022.07.2	https://www.rstudio.com/products/rstudio/download/
biomaRt	2.52.0	https://bioconductor.org/packages/release/bioc/html/biomaRt.html
cowplot	1.1.1	https://cran.r-project.org/web/packages/cowplot/
dittoSeq	1.8.1	https://bioconductor.org/packages/release/bioc/html/dittoSeq.html
dplyr	1.0.10	https://dplyr.tidyverse.org/
escape	1.6.0	https://github.com/ncborcherding/escape
ggplot2	3.3.6	https://ggplot2.tidyverse.org/
GSEABase	1.58.0	https://bioconductor.org/packages/release/bioc/html/GSEABase.html
htmlwidgets	1.5.4	https://www.htmlwidgets.org/
Matrix	1.5-1	https://cran.r-project.org/web/packages/Matrix/index.html
patchwork	1.1.2	https://patchwork.data-imaginist.com/
plotly	4.10.0	https://plotly.com/r/
reticulate	1.26	https://rstudio.github.io/reticulate/
Seurat	4.2.0	https://satijalab.org/seurat/
SeuratDisk	0.0.0.9020	https://github.com/mojaveazure/seurat-disk
ggalt	0.4.0	https://yonicd.github.io/ggalt/index.html
CellChat	1.5.0	https://github.com/sqjin/CellChat

2

3

1 **Table S2. Primary antibodies for immunohistochemistry**

Antibody	Concentration	Vendor	Catalog #
Chicken Anti-mCherry	1:500	Abcam	ab205402
Chicken Anti-GFP	1:50	enQuire BioReagents	NC1666473
Rabbit Anti-RBPMS	1:300	GeneTex	GTX118619
Mouse Anti-Thy1	1:400	Serotec	MCA02R
Rabbit Anti-Map2	1:250	Biolegend	840601
Anti-Osteopontin	1:250	Hybridoma Bank	MPIIIB10(1)
Rabbit Anti-Melanopsin	1:400	Santa Cruz	sc-32870
Mouse B3-tubulin	1:500	Sigma Aldrich	T8660
Mouse Brn3a	1:500	Millipore	MAB1585

2

3

4